

# Very early multi-color observations of the plateau phase of GRB 041006 afterglow

Y URATA<sup>1,2</sup>, K.Y. HUANG<sup>3</sup>, Y.L. QIU<sup>4</sup>, J. HU<sup>4</sup>, P.H. KUO<sup>3</sup>, T. TAMAGAWA<sup>2</sup>, W.H. IP<sup>3</sup>, D. KINOSHITA<sup>3</sup>, H. FUKUSHI<sup>5</sup>, M. ISOGAI<sup>6</sup>, T. MIYATA<sup>6</sup>, Y. NAKADA<sup>6</sup>, T. AOKI<sup>6</sup>, T. SOYANO<sup>6</sup>, K. TARUSAWA<sup>6</sup>, H. MITO<sup>5</sup>, K. ONDA<sup>1</sup>, M. IBRAHIMOV<sup>7</sup>, A. POZANENKO<sup>8</sup> and K. MAKISHIMA<sup>2,9</sup>

urata@heal.phy.saitama-u.ac.jp

## ABSTRACT

Observations of the optical afterglow of GRB 041006 with the Kiso Observatory 1.05 m Schmidt telescope, the Lulin Observatory 1.0 m telescope and the Xinglong Observatory 0.6 m telescope. Three-bands ( $B$ ,  $V$  and  $R$ ) of photometric data points were obtained on 2004 October 6, 0.025–0.329 days after the burst. These very early multi band light curves imply the existence of a color dependent plateau phase. The  $B$ -band light curve shows a clear plateau at around 0.03 days after the burst. The  $R$  band light curve shows the hint of a plateau, or a possible slope change, at around 0.1 days after the burst. The overall behavior of these multi-band light curves may be interpreted in terms of the sum of two separate components, one showing a monotonic decay the other exhibiting a rising and a falling phase, as described by the standard afterglow model.

---

<sup>1</sup>Department of Physics, Saitama University, Shimo-Okubo, Saitama, 338-8570, Japan

<sup>2</sup>RIKEN (Institute of Physical and Chemical Research), 2-1 Hirosawa, Wako, Saitama 351-0198, Japan

<sup>3</sup>Institute of Astronomy, National Central University, Chung-Li 32054, Taiwan, Republic of China

<sup>4</sup>National Astronomical Observatories, Chinese Academy of Sciences, Beijing 100012, China

<sup>5</sup>Institute of Astronomy, University of Tokyo, 2-21-1 Osawa, Mitaka, Tokyo 181-0015, Japan

<sup>6</sup>Kiso Observatory, Institute of Astronomy, The University of Tokyo, Mitake-mura, Kiso-gun, Nagano 397-0101, Japan

<sup>7</sup>Ulugh Beg Astronomical Institute, Tashkent 700052, Uzbekistan

<sup>8</sup>Space Research Institute, 84/32 Profsoyuznaya Str, Moscow 117997, Russia

<sup>9</sup>Department of Physics, University of Tokyo, 7-3-1 Hongo, Bunkyo-ku, Tokyo 113-0033, Japan

*Subject headings:* Gamma-ray Bursts: afterglow

## 1. Introduction

Based on the standard afterglow model (e.g. Sari, Piran and Narayan 1998), an optical light curve can be expected to consist of a combination of four power-law segments, with connections at certain break frequencies. The break frequencies are the self-absorption frequency ( $\nu_{sa}$ ), the typical frequency ( $\nu_m$ ) and the cooling frequency ( $\nu_c$ ). Before the *HETE-2* era, almost all GRB light curves showed only the  $\nu > \nu_c$  segment characterized by a single declining or achromatic break. Note that the standard afterglow model predicts the existence of a peak at an early time when the typical synchrotron  $\nu_m$  frequency crosses into the optical frequency. Before the peak time ( $\nu_{opt} < \nu_m$ ), the luminosity increases proportional to  $t^{1/2}$ , until reaching the maximum flux  $F_{max}$  at  $\nu = \nu_m$ ; the subsequent decay of the luminosity is proportional to  $t^{3(1-p)/4}$ , where  $p$  is the index of the power-law distribution of energetic electrons accelerated at the shock. Since the break time varies with the frequency, multi-color observations of the very early afterglow are required, so as to catch  $\nu_m$  in the optical wavelength. Up to now, there have only been a few cases (such as GRB 021004; Urata et al 2005a) for which early time multi-color data are available.

GRB 041006 was detected with *HETE-2* at 12:18:08 UT on 2004 October 06. The Wide-Field X-ray Monitor (WXM; Shirasaki et al 2003) localized the burst in real time, resulting in a GCN alert 42 seconds after the burst trigger. The flight error region was a circle with a 14' radius (90% confidence level) centered at  $\alpha^{2000} = 00^h54^m54^s$ ,  $\delta^{2000} = 01^\circ18'37''$ . Spectral analysis showed the 2-30 keV fluence of this event to be  $5 \times 10^{-6}$  erg/cm<sup>2</sup> and the 30-400 keV fluence to be  $7 \times 10^{-6}$  erg/cm<sup>2</sup>: the ratio between these two values means that it can be classified as an “X-ray rich GRB”. The light curve shape of the gamma-ray pulse of GRB 041006 is very similar to that of GRB 030329 but, its spectral characteristics are 20 times fainter. GRB 041006 shows a soft precursor before the main gamma-ray pulse (Galassi et al. 2004). At 1.4 hours after the burst, the optical afterglow was found within the 14'-radius error circle at the following coordinates:  $\alpha^{2000} = 00^h54^m50^s.17$ ,  $\delta^{2000} = 01^\circ14'07''$  (Da Costa et al. 2004). The redshift was determined by Price et al. (2004) using the Gemini North telescope to be  $z = 0.716$ .

## 2. Observations

The follow-up observations of the GRB 041006 optical afterglow at the Kiso, Lulin and Xinglong Observatories were carried out within the framework of the East Asia Follow-up Observation Network (EAFON, Urata et al. 2005b). The 1.05 m Schmidt telescope and a  $2k \times 2k$  CCD camera at the Kiso observatory were used to make 300 sec exposure  $B$ ,  $V$ , and  $R$  band imaging observations, starting at 12:51 UT on 2004 October 6 (0.009 days after the burst). The field of view is  $51'.2 \times 51'.2$ , and the pixel size is  $1''.5$  square. Before receiving the report by Da Costa et al. (2004), we had attempted to cover the entire *HETE-2* error region. We made  $B$ ,  $V$ , and  $R$  band imaging observations of 300 sec exposure each. The afterglow was clearly detected in all bands. In order to image simultaneously the optical afterglow and several Landolt standard stars in SA92 (Landolt 1992), we pointed the telescope 5 arcmin to the east (Figure 1).

The  $R$  band observations were performed using the 0.6 m telescope at the Xinglong Observatory, starting at 2004 October 6 (14:33 UT; 0.094 days after the burst). The field of view is  $10'.1 \times 10'.1$ , and the pixel size is  $0''.47$  square. The  $B$  and  $R$  band observation of the afterglow was also performed with the Lulin-One-meter-Telescope (Kinoshita et al. 2005) on the night of October 6 (0.320 – 0.329 days after the burst). Additional  $B$ ,  $V$ ,  $R$  and  $I$  band observations were made by the Maidnak 1.5 m telescope on October 6. The time coverage of the observations was from 0.149 to 0.188 days after the burst.

## 3. Analysis

The data reduction was carried out using the standard package NOAO IRAF package. We performed the bias-subtraction and flat-fielding correction using the appropriate calibration data. We calibrated the flux zero-point of our images through a comparison with the SA92 standard star field. We also performed cross calibrations of our photometric results using several field stars for which the magnitudes have been calibrated by Henden (2004). The difference of photometric zero points between our SA92 and Henden’s field photometry is within 0.04 mag. Aperture photometry for all the data was performed using the APPHOT package of IRAF. The photometric results are summarized in Table 1.

## 4. Results

### 4.1. Light curves

The multi-band light curves of the GRB 041006 afterglow are shown in Figure 2. In addition to our  $B$ ,  $V$  and  $R$  band data, there are several unfiltered observations, the  $R$  band data points reported in the GCN Circulars (Yost et al. 2004; Ayani & Yamaoka 2004; Fugazza et al. 2004; Monfardini et al. 2004; Misra & Pandey 2004; Kahharov et al. 2004; Kinugasa & Torii 2004), and a number of published  $R$  and  $V$  band data points (Soderberg et al. 2005; Stanek et al. 2005) were included in Figure 2. The  $B$ -band light curve showed a clear plateau at around 0.03 days after the burst, although its behavior in earlier epochs remains unknown. Interestingly, the  $R$  band light curve shows a hint of a plateau, or a possible slope change, around 0.1 days after the burst. These observational results indicate that the  $B$ ,  $V$  and  $R$  band photometric points obtained by EAFON play an important role in characterizing the temporal evolution of the afterglow.

As is obvious in the Figure 2, the single power law fit ( $\alpha = -0.95$ ,  $\chi^2/\nu = 5.76$  with  $\nu=56$ ) of the  $R$  band light curve is poorly described. It is also unlikely that the  $V$  band light curve can be described with the single power law ( $\alpha = -0.72$ ,  $\chi^2/\nu = 1.54$  with  $\nu=9$ ). On the other hand, the data subsets at  $t < 0.04$  days and  $t > 0.15$  days can be described successfully by two separate single power-law models. For the  $R$  band, we have obtained  $\alpha = -0.91 \pm 0.12$  with  $\chi^2/\nu = 0.30$  for  $\nu = 2$  before 0.04 days, and  $\alpha = -1.12 \pm 0.02$  with  $\chi^2/\nu = 1.44$  for  $\nu = 48$  after 0.15 days; for the  $V$  band  $\alpha = -0.59 \pm 0.03$  with  $\chi^2/\nu = 0.41$  for  $\nu = 3$  before 0.04 day, and  $\alpha = -1.41 \pm 0.30$  with  $\chi^2/\nu = 0.19$  for  $\nu = 1$  after 0.15 days. From this point of view, the overall behavior of these multi band light curves may then be understood as the sum of two separate components, one showing a monotonic decay with the other having a rising and a falling phase.

### 4.2. Color change of the afterglow

The photometric results were corrected for Galactic reddening, using the reddening map of Schlegel, Finkbeiner, & Davis (1998). The Galactic reddening toward the burst is  $E(B - V) = 0.022$ , which implies a Galactic extinction of  $A_B = 0.094$  and  $A_R = 0.058$ . Although the light curves in Figure 2 suggest a significant color change within  $< 0.1$  days, our data coverage is insufficient to make a conclusion about such a possibility. Accordingly, for simplicity's sake we assume that at  $t > 0.15$  days the power-law spectrum of the afterglow has a constant index. The observed color,  $B - R = 0.83 \pm 0.28$  mag, then indicates a spectral index of  $\beta \sim -1.24 \pm 0.42$  in terms of  $f(\nu) \propto \nu^\beta$ . This is close to the value of  $\beta = -1.07 \pm 0.02$ ,

which is predicted by the spherically symmetric model of Sari, Piran, & Halpern (1999) in the regime of  $\nu_c < \nu_{opt}$  in combination with the measured  $\alpha = -1.118 \pm 0.016$ .

## 5. Discussion

We observed the GRB 041006 optical afterglow from the very early phase ( $\sim 0.03$  days after the burst) in three bands. Although the relatively early phase of a dozen afterglows such as GRB 990123 (Akerlof et al. 1999), multi-color observations of very early optical afterglow are still rare. In the GRB 021004 case, the very early optical afterglow shows a clear achromatic re-brightening phase which peaks was at around  $\sim 0.07$  days (Urata et al. 2005b). On the other hand, the afterglow behavior of GRB 041006 depends on its color. The  $B$  band light curve shows a clear plateau at around 0.03 days after the burst, although its behavior in earlier epochs remains unknown. The  $R$  band light curve shows the hint of a plateau, or a possible slope change, around 0.1 days after the burst.

Several models, based on the standard afterglow model, can be used to explain the variability in the light curve, such as the variable external density (e.g. Lazati et al. 2002), refreshed shock (Rees & Mészáros 1998; Kumar & Piran 2000a; Sari & Mészáros 2000), and patchy shell models (Kumar & Piran 2000b). To explain the present multi-band light curves, these models require similar temporal behavior in each band. If the light curve of GRB 041006 does not show a color change, it should have two bumps with almost the same amplitudes. The patchy shell model is not suitable to explain current light curves in this case. This is because the model predicts that the amplitude of the fluctuations in the afterglow light curve is expected to decrease with time proportional to the Lorentz factor.

The suggested second component may be identified with the brightening phase of Sari et al.’s standard afterglow model (1998) which predicts the evolution to consist of four phases involving a convex-shaped period; the brightening phase can be expressed with a power-law index of 0.5. To describe the plateau phase together with the monotonically decreasing first component, we use the single power law, plus a smoothly broken power law function expressed as

$$F_\nu(t) = \frac{F_\nu^*}{[(t/t_b)^{\alpha_1} + (t/t_b)^{\alpha_2}]}, \quad (1)$$

with  $\alpha_1$  fixed at 0.5 after Sari et al. (1998). We obtain an acceptable fit for the  $R$  band light curve with  $\alpha = -1.07 \pm 0.01$ ,  $\alpha_2 = -1.49 \pm 0.03$  and  $t_b = 0.143 \pm 0.012$  ( $\chi^2/\nu = 1.19$  with  $\nu = 66$ ). We also fit the  $B$  and  $V$  band light curves with the same function. For better constraints, we fix the  $\alpha_1 = -1.0$  for  $B$  band and  $\alpha_2 = -1.4$  of the  $V$  band. Due to the lack

of data points for the first components in the  $B$  band, and the former components in the  $V$  band., these vales come from the result of  $R$  band fitting. For the  $B$  band, we obtained  $\alpha_2 = -1.47 \pm 0.07$  and  $t_b = 0.0675 \pm 0.005$  ( $\chi^2/\nu = 0.47$  with  $\nu = 7$ ); for the  $V$  band,  $\alpha = -1.08 \pm 0.02$  and  $t_b = 0.073 \pm 0.006$  ( $\chi^2/\nu = 0.83$  with  $\nu = 8$ ). In Figure 2, these best fit functions are superposed on the  $B$ ,  $V$  and  $R$  band data points. Based on the equation (Sari et al. 1998)

$$\nu_m = 5.7 \times 10^{14} \epsilon_B^{1/2} \epsilon_e^2 E_{52}^{1/2} t_d^{-3/2} \text{ Hz}, \quad (2)$$

we can estimate the strength parameter of the magnetic field  $\epsilon_B$  and/or the injected electrons parameter  $\epsilon_e$  as follows;  $\epsilon_B^{1/2} \epsilon_e^2 = 4.1 \times 10^{-3}$ . This value is consistent with the result of Panaitescu & Kumar (2001, 2002) which was estimated from late-time multi-frequency afterglow observations.

About the first component, the decay index is  $\alpha = -0.92$  and the back-extrapolated power-law function can successfully account for the point at 14.4 min after the burst observed by ROTSE-III (Yost et al. 2004). The temporal index is considered to be directly related to the prompt emission, as observed in the case of GRB 990123 (Akerlof et al. 1999) or GRB 030418 (Rykoff et al. 2004). However, the temporal index is inconsistent with the values ( $-0.5$  or  $-2$ ) predicted by a reverse shock model (Kobayashi 2000). Thus the first component is not likely to be an optical flash, such as is the case for GRB 990123. Considering the above discussions one of possible explanation is that these emissions come from multiple jets and/or sub-jets (Nakamura 2000, Yamazaki et al. 2004). In the multiple jet case, the former emissions and the latter components are caused by narrower and wider jets, respectively.

## 6. Conclusion

Thanks to our EAFON observations, we have obtained early B, V and R band possible re-brightening episode for GRB 041006. While there are several other afterglows similar to GRB 050319 (Wozniak et al 2005; Huang et al 2006) and GRB 050525a (Klotz et al. 2005) for which the early optical behaviors may possibly be similar to that of GRB 041006, their physical mechanism is not clear, due to the general lack of color/spectrum information on the early optical afterglows. The present work has provided some hints for the current shallow decaying of the X-ray and optical behaviors.

We thank the staff and observers at the Kiso, Lulin and XingLong observatories for the

various arrangements. Y.U acknowledges support from the Japan Society for the Promotion of Science (JSPS) through JSPS Research Fellowships for Young Scientists. This work is also partly supported by grants NSC 94-2752-M-008-001-PAE, NSC 94-2112-M-008-002, and NSC 94-2112-M-008-019.

## REFERENCES

- Akerlof, C., et al. 1999, *Nature*, 398, 400
- Ayani, K., & Yamaoka, H. 2004, *GCN Circ.* 2779 154
- Da Costa, G., Novel, G. & Price, P.A. 2004, *GCN Circ* 2765
- Fugazza, D. et al. 2004, *GCN Circ* 2782
- Galassi, M., et al. 2004, *GCN Circ* 2770
- Henden, A., 2004, *GCN Circ* 2801
- Huang, K. Y., et al. 2006, *ApJL* accepted
- Kahharov, B., Asfandiyarov, I., Ibrahimov, M., Sharapov, D., Pozanenko, A., Rumyantsev, V. & Beskin, G. 2004, *GCN Circ* 2775
- Kinugasa, K., & Torii, K. 2004, *GCN Circ* 2832
- Kinoshita, D., et al. 2005, *ChJAA*, 5, 315
- Klotz, A., Boeř, M., Atteia, J.D., Stratta, G., Behrend, R., Malacrino, F. & Damerdjı, Y. 205, *A&A*, 439, 35
- Kobayashi, S. 2000, *ApJ*, 545, 807
- Kumar, P., & Piran, T. 2000a, *ApJ*, 532, 286
- Kumar, P., & Piran, T. 2000b, *ApJ*, 535, 152
- Landolt, A. U. 1992, *AJ*, 104, 340
- Lazzati, D., Rossi, D., Covino, S., Ghisellini, G & Malesani, D. 2002 *A&A*, 396, L5
- Misra, K. & Pandey, S.B. 2004, *GCN Circ* 2794
- Monfardini, A., et al. 2004, *GCN Circ* 2790

- Nakamura, T. 2000, *ApJ*, 534, 159
- Panaiteescu, A., & Kumar, P. 2001, *ApJ*, 560, L49
- Panaiteescu, A., & Kumar, P. 2002, *ApJ*, 571, 779
- Rees, M. J., & Mešzaáros, P. 1998, *ApJ*, 496, L1
- Price, P.A. 2004, *GCN Circ* 2791
- Rykoff, E.S., et al. 2004, *ApJ*, 601, 1013
- Sari, R., Piran, T. & Narayan, R. 1998, *ApJ*, 497, L17
- Sari, R., Piran, T. & Halpwrn, J. P. 1999, *ApJ*, 519, L17
- Sari, R., & Mészáros, P. 2000, *ApJ*, 535, L33
- Schlegel, D. J., Finkbeiner, D. P. & Davis, M. 1998, *ApJ*, 500, 525
- Shirasaki, Y., et al. 2003, *PASJ*, 55, 1033
- Soderberg, A. et al. 2005, *ApJ*, 636, 391
- Stanek, K. Z. et al. 2005, *ApJ*, 636, L5
- Urata, Y., et al. 2003, *ApJ*, 595, L21
- Urata, Y., et al. 2004, *ApJ*, 601, L17
- Urata, Y., et al. 2005a, *Il Nuovo CIMENTO*, 28, 775
- Urata, Y., et al. 2005b, *Nuovo CIMENTO*, 28, 779
- Wozniak, P. R., Vestrand, W. T., Wren, J. A., White, R. R., Evans, S. M., Casperson, D.  
2005, *ApJ*, 627, L13
- Yamazaki, R., Ioka, K & Nakamura, T. 2004, *ApJ*, 607, L103
- Yost, S., Smith, D.A., Rykoff, E.S. & Swan, H. 2005, *GCN Circ.* 2776



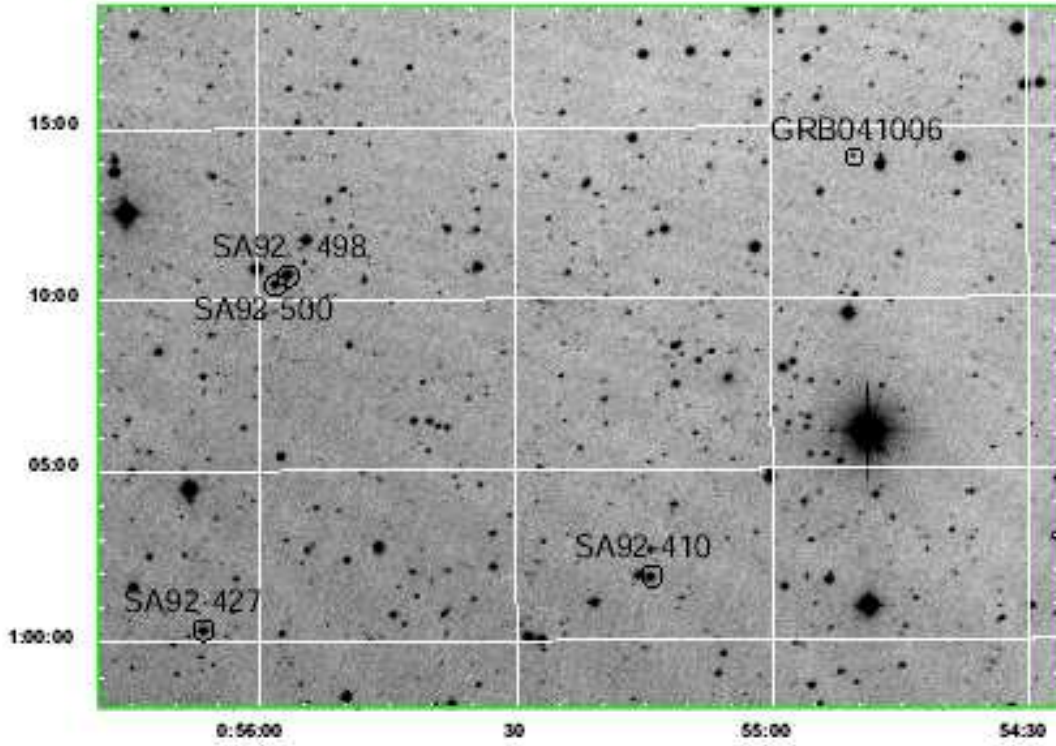


Fig. 1.— An  $R$  band image of the GRB 041006 field taken at the Kiso observatory. The circles indicate the afterglow and standard stars. North is up; east is left.

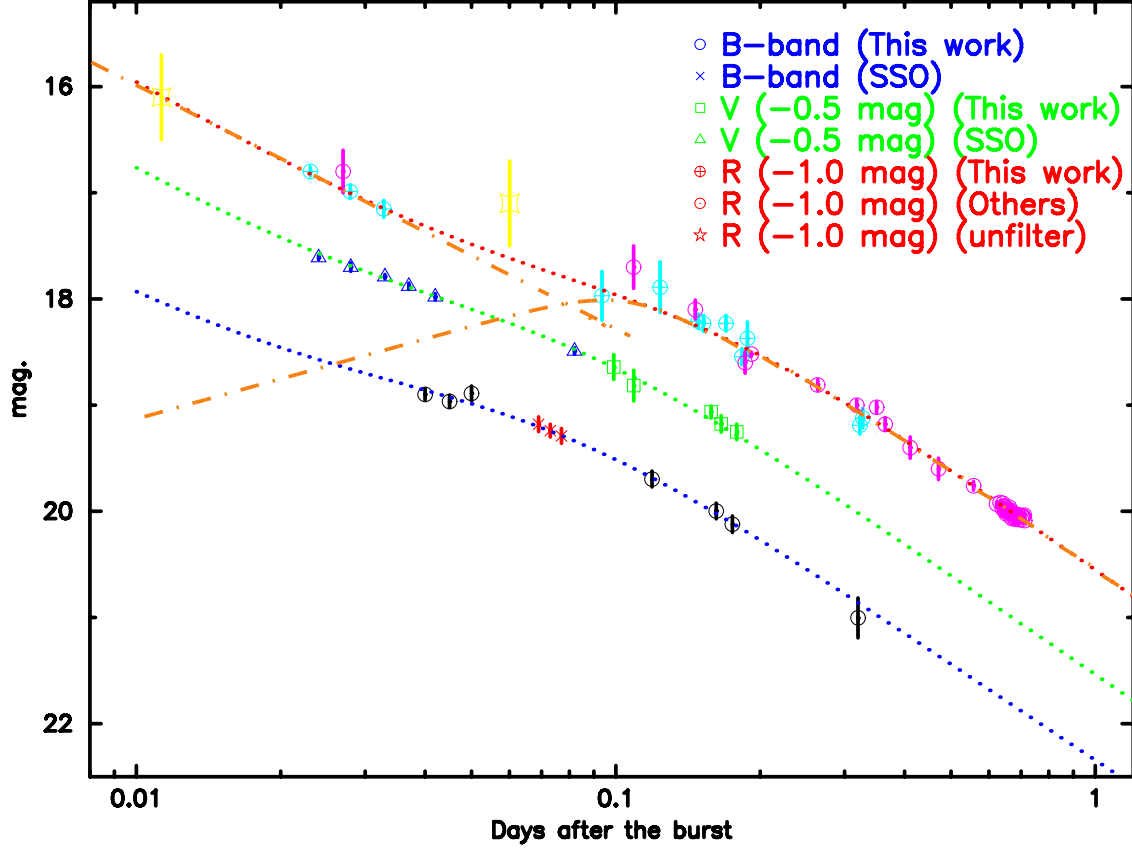


Fig. 2.—  $B$ ,  $V$  and  $R$  band light curves produced based on the Kiso, Lulin and Beijing results together with SSO(Soderberg et al 2005), MMT(Stanek 2005) and several GCNs. The dotted lines indicate the best fit model functions described in the text. The dashed lines indicate the model components of the best fit function for the  $R$  band lightcurve.

Table 1: Log of follow-up observations of the afterglow of GRB 041006.

Date	Start Time(UT)	Delay (days)	Filter	Exposure (s)	mag	Site
2004-10-06	13:13:04	0.040	<i>B</i>	300 s $\times$ 1	18.900 $\pm$ 0.055	Kiso
2004-10-06	13:20:05	0.045	<i>B</i>	300 s $\times$ 1	18.965 $\pm$ 0.058	Kiso
2004-10-06	13:27:05	0.050	<i>B</i>	300 s $\times$ 1	18.890 $\pm$ 0.070	Kiso
2004-10-06	15:07:22	0.119	<i>B</i>	300 s $\times$ 1	19.696 $\pm$ 0.074	Kiso
2004-10-06	16:09:02	0.162	<i>B</i>	300 s $\times$ 1	19.997 $\pm$ 0.074	Mt. Maidanak
2004-10-06	16:27:48	0.175	<i>B</i>	300 s $\times$ 1	20.122 $\pm$ 0.078	Mt. Maidanak
2004-10-06	19:57:08	0.320	<i>B</i>	300 s $\times$ 1	21.004 $\pm$ 0.188	Lulin
2004-10-06	14:38:52	0.099	<i>V</i>	300 s $\times$ 1	19.141 $\pm$ 0.117	Kiso
2004-10-06	14:52:56	0.109	<i>V</i>	300 s $\times$ 1	19.316 $\pm$ 0.145	Kiso
2004-10-06	16:03:40	0.158	<i>V</i>	240 s $\times$ 1	19.564 $\pm$ 0.057	Mt. Maidanak
2004-10-06	16:14:57	0.166	<i>V</i>	240 s $\times$ 1	19.677 $\pm$ 0.078	Mt. Maidanak
2004-10-06	16:33:28	0.179	<i>V</i>	300 s $\times$ 1	19.752 $\pm$ 0.074	Mt. Maidanak
2004-10-06	12:51:20	0.025	<i>R</i>	300 s $\times$ 1	17.799 $\pm$ 0.040	Kiso
2004-10-06	12:58:21	0.030	<i>R</i>	300 s $\times$ 1	17.988 $\pm$ 0.063	Kiso
2004-10-06	13:05:23	0.035	<i>R</i>	300 s $\times$ 1	18.152 $\pm$ 0.080	Kiso
2004-10-06	14:32:51	0.094	<i>R</i>	120 s $\times$ 1	18.97 $\pm$ 0.23	Beijing
2004-10-06	15:16:15	0.124	<i>R</i>	120 s $\times$ 1	18.89 $\pm$ 0.24	Beijing
2004-10-06	15:49:32	0.149	<i>R</i>	180 s $\times$ 1	19.211 $\pm$ 0.067	Mt. Maidanak
2004-10-06	15:54:56	0.152	<i>R</i>	180 s $\times$ 1	19.231 $\pm$ 0.075	Mt. Maidanak
2004-10-06	16:19:59	0.170	<i>R</i>	180 s $\times$ 1	19.229 $\pm$ 0.074	Mt. Maidanak
2004-10-06	16:39:30	0.183	<i>R</i>	300 s $\times$ 1	19.544 $\pm$ 0.076	Mt. Maidanak
2004-10-06	16:46:28	0.189	<i>R</i>	300 s $\times$ 1	19.371 $\pm$ 0.156	Mt. Maidanak
2004-10-06	20:02:54	0.324	<i>R</i>	300 s $\times$ 1	20.349 $\pm$ 0.090	Lulin
2004-10-06	20:09:25	0.329	<i>R</i>	300 s $\times$ 1	20.314 $\pm$ 0.092	Lulin